OXFORD

Utility of In Vivo Magnetic Resonance Imaging Is Predictive of Gestational Diabetes Mellitus During Early Pregnancy

Brian Lee,[1] Carla Janzen,[2] Holden Wu,[3] Sitaram S. Vangala,[4] Sherin U. Devaskar,[1] and Kyunghyun Sung[3]

[1]Department of Pediatrics, David Geffen School of Medicine, University of California, Los Angeles, CA 90095, USA
[2]Department of Obstetrics and Gynecology, Division of Perinatology Maternal Fetal Medicine, David Geffen School of Medicine at UCLA, Los Angeles, CA 90095, USA
[3]Department of Radiological Sciences, David Geffen School of Medicine, University of California, Los Angeles, CA 90095, USA
[4]Department of Medicine, David Geffen School of Medicine, University of California, Los Angeles, CA 90095, USA
Correspondence: Sherin U. Devaskar, MD, Department of Pediatrics, David Geffen School of Medicine, University of California Los Angeles, 10833, Le Conte Avenue, Los Angeles, CA 90095-1752, USA. Email: sdevaskar@mednet.ucla.edu.

Abstract

Context: Gestational diabetes (GDM) imposes long-term adverse health effects on the mother and fetus. The role of magnetic resonance imaging (MRI) during early gestation in GDM has not been well-studied.

Objective: To investigate the role of quantitative MRI measurements of placental volume and perfusion, with distribution of maternal adiposity, during early gestation in GDM.

Methods: At UCLA outpatient antenatal obstetrics clinics, ~200 pregnant women recruited in the first trimester were followed temporally through pregnancy until parturition. Two placental MRI scans were prospectively performed at 14 to 16 weeks and 19 to 24 weeks gestational age (GA). Placental volume and blood flow (PBF) were calculated from placental regions of interest; maternal adiposity distribution was assessed by subcutaneous fat area ratio (SFAR) and visceral fat area ratio (VFAR). Statistical comparisons were performed using the two-tailed *t* test. Predictive logistic regression modeling was evaluated by area under the curve (AUC).

Results: Of a total 186 subjects, 21 subjects (11.3%) developed GDM. VFAR was higher in GDM vs the control group, at both time points ($P < 0.001$ each). Placental volume was greater in GDM vs the control group at 19 to 24 weeks GA ($P = 0.01$). Combining VFAR, placental volume and perfusion, improved the AUC to 0.83 at 14 to 16 weeks (positive predictive value [PPV] = 0.77, negative predictive value [NPV] = 0.83), and 0.81 at 19 to 24 weeks GA (PPV = 0.73, NPV = 0.86).

Conclusion: A combination of MRI-based placental volume, perfusion, and visceral adiposity during early pregnancy demonstrates significant changes in GDM and provides a proof of concept for predicting the subsequent development of GDM.

Key Words: gestational diabetes, placenta MRI, maternal adiposity, visceral and subcutaneous fat, prediction modeling

Gestational diabetes (GDM) is defined as diabetes mellitus that is first identified during pregnancy. There is an epidemic of GDM that includes well-resourced and poor-resourced countries worldwide. The prevalence of GDM within the United States is estimated at 6.0% (1), representing an increase from 3.7% since 2000 (2). Mothers with GDM have an increased risk of subsequently developing type 2 diabetes (3) and cardiovascular disease (4). Babies born to mothers with GDM have an increased risk for macrosomia (5), prematurity (6), being born small for gestational age, certain perinatal complications (7), and childhood obesity (8) associated with type 2 diabetes mellitus presenting at an early age.

Early development of GDM may confer an increased risk of metabolic disease to both the mother and the offspring. This may be related to maternal GDM-induced aberrancy in placental function. Placental perfusion is pathologically reduced in GDM pregnancies due to thickening of the trophoblastic basement membrane (9), increased inflammatory cytokine release by placental macrophages (10), and edema of the

villous stromal layer (11). Reduced placental perfusion is counterproductive to the increased fetal oxygen demand due to fetal hyperinsulinemia seen in GDM (10). Ultrasound Doppler measurements of placental perfusion early in gestation have been performed by means of the uterine artery pulsatility index (UtA-PI) but has not been extensively studied in the context of placental changes in GDM, although a prior study found that early-gestation measurements of UtA-PI did not differ in patients who developed GDM (12). However, UtA-PI assesses resistance to blood flow and does not directly measure placental perfusion or function. Such changes in placental function may be better assessed directly using the high-resolution noninvasive modality of recently developed free-breathing magnetic resonance imaging (MRI) measurements of placental perfusion. Our group and others have demonstrated the utility of novel MRI techniques in measuring placental function during early pregnancy (13). While more recently there is increasing clinical familiarity in undertaking MRI studies for the purpose of diagnosing fetal structural

anomalies and certain placental structural aberrations (eg, placental accreta spectrum), its use early in pregnancy for assessing placental function is novel.

The current screening test for GDM is an oral glucose tolerance test (OGTT) performed, at 24 to 28 weeks gestational age (GA). Due to the clinical implications of GDM for both mother and fetus, improved early-gestation screening besides an earlier undertaking of OGTT, with associated inaccuracies, is warranted to identify mothers at risk for developing GDM. Earlier OGTT screening prior to 24 weeks GA has been suggested, in particular for obese women with additional risk factors for developing GDM [14]. However, there continues to be an ongoing discussion regarding the ideal screening algorithm [15]. The few randomized control trials of early GDM screening have not shown any difference or improvement in perinatal outcomes [16–18]. This stems from uncertainty with respect to ideal glucose concentration cutoff values to be used during early pregnancy and other factors that impinge upon the accuracy of OGTTs during this period of pregnancy [15, 16].

To this end, many clinical investigations have focused on clinical and biochemical features besides the OGTT in defining a high-risk panel of predictors to help risk-stratify patients with a high probability of developing GDM subsequently [19, 20]. Clinical reliance is routinely placed on pre-pregnancy body mass index (BMI) measurements in predicting complications, but this suffers from the inability to differentiate between subcutaneous and visceral fat deposition. Pre-pregnancy BMI measurements do not provide insights into fat distribution nor allow region-specific assessment of accumulating fat mass during pregnancy.

The overall risk of insulin resistance and cardiovascular and metabolic disease is closely correlated with increased visceral fat deposition [21]. Women with GDM have been shown to have increased visceral adiposity, as assessed directly by cross-sectional measurements of fat deposits obtained at cesarian sections [22]. In addition, measurements of maternal adiposity by ultrasound have shown promise in the prediction of GDM, particularly when measuring visceral fat distribution [21, 23–25]. However, there is inconsistency in the methods employed among studies measuring visceral fat thickness [21, 23–25]. While MRI has been widely employed to analyze fat content, including differences in subcutaneous and visceral fat [26], there is scant literature on its use in relation to GDM, particularly in early pregnancy, with the possibility of detection and perhaps prediction. Early-gestation MRI can further shed light upon the interrelationship between the state of maternal insulin resistance seen by the visceral fat distribution and the impact on placental volume and the ultimate function of perfusion.

Based on this collection of existing information, we hypothesized that patients who later develop GDM will show differences in placental function and maternal adiposity in early pregnancy, compared with patients who have a normal pregnancy. To test this hypothesis, we aim to investigate quantitative measures of placental volume and perfusion along with distribution of maternal adiposity, measured by second-trimester placenta MRI to evaluate differences between a normal pregnancy and a pregnancy complicated by GDM. Early detection of differential features may aid in the introduction of timely intervention and treatment of GDM, with an attempt at predictability, having an impact on health outcomes for both the mother and her fetus.

Methods

Patient Recruitment and Data Collection

This prospective study was approved by the University of California Los Angeles (UCLA) Institutional Review Board, and all subjects provided written informed consent upon recruitment. The women recruited in this study were subjects of the National Institutes of Health (NIH)-initiated Human Placenta Project [27], which aims to understand how placental structure and function change in vivo throughout pregnancy, and how these alterations may lead to different maternal and fetal outcomes. Therefore, the study enrollment was based on the primary objective of developing and evaluating novel MRI technologies to perform safe and non-invasive real-time assessment of placental structure and function.

Without preselection for clinical high-risk factors, a total of 199 women were recruited from established UCLA antenatal clinics and consented in early pregnancy between February 2017 and February 2019 for participation in the study at UCLA Ronald Reagan Medical Center. Inclusion criteria were a gestational age of less than 14 weeks, maternal age of more than 18 years, pregnancy not carrying twins, the absence of fetal chromosomal or structural abnormalities, the ability to provide consent, a nonsmoker, and planning to deliver at the same local institution. Exclusion criteria included maternal age of less than 18 years, fetal malformation evident before enrollment or a known fetal chromosomal abnormality, twin pregnancy, a plan to terminate the pregnancy, or inability to provide consent.

At recruitment, data including prior pregnancy history, pre-pregnancy body mass index (BMI), and age, were recorded. Maternal pre-pregnancy BMI was self-reported during the initial study visit. The pregnancy course was then prospectively followed at 4 study visits, which were first at a gestational age of 11 to 14 weeks, second at 20 to 29 weeks, third at 36 weeks, and fourth at parturition (Fig. 1A). No other biochemical data were available other than glucose screens and any other testing that was clinically indicated. The diagnosis of GDM was part of the routine clinical care and recorded at the second and third study visits. Neonatal outcomes were also recorded at delivery, and neonates were followed postnatally up to 16 weeks after birth.

GDM at our institution was defined as glucose intolerance first diagnosed during pregnancy, using a 50-gram glucose challenge test as an initial screen at 24 to 28 weeks gestational age. If the venous blood glucose level 1 hour after the 50-gram challenge was greater than 135 mg/dL, the subject would undergo a diagnostic 100-gram fasting glucose tolerance test; an abnormal result would lead to the diagnosis of GDM based on the American College of Obstetricians and Gynecologists 2018 practice bulletin [14]. Neonatal outcomes were recorded at birth and at 3 visits until 16 weeks of postmenstrual age.

In terms of BMI in kg/m^2, a BMI less than 18.5 was considered underweight; greater than 18.5 but less than 25 was normal weight; greater than or equal to 25 but less than 30 was overweight; and greater than or equal to 30 was obese.

MRI Acquisition and Image Analysis

While the secondary analysis of assessing GDM was pre-planned, the study required developing and testing the
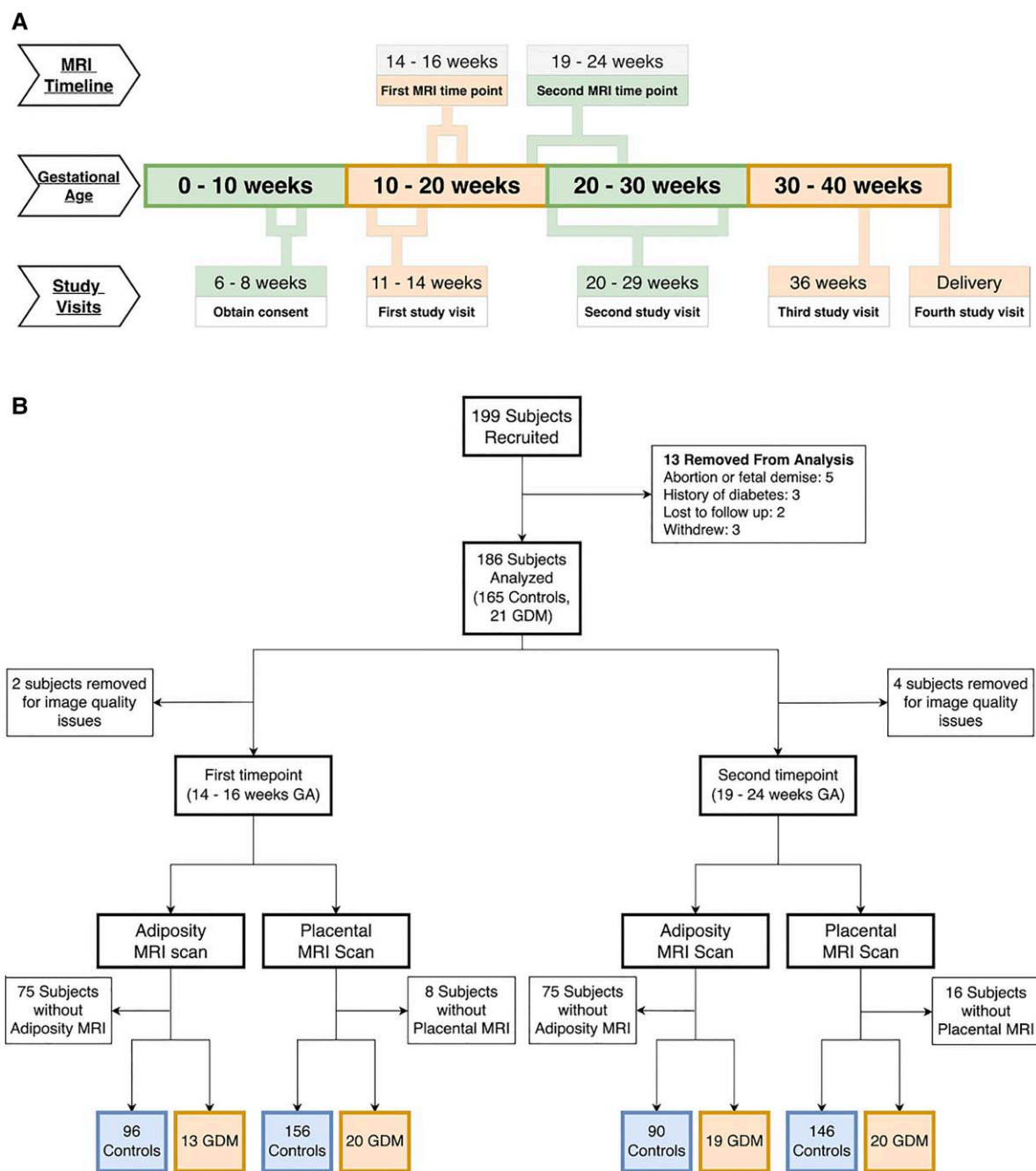
Figure 1. A. Study timeline. This figure depicts the study timeline. The middle row (Gestational Age) represents the temporal course of the pregnancy. The top row (MRI Timeline) depicts the 2 MRI time points, at 14-16 weeks and 19-24 weeks. The bottom row (Study Visits) depicts the timeline of recruitment (at 6-8 weeks) and the 4 study visits planned for each subject (at 11-14 weeks, 20-29 weeks, 36 weeks, and at delivery). Recruitment flowchart. Abbreviations: D&C, dilation and curettage; GA, gestational age; GDM, gestational diabetes; MRI, magnetic resonance imaging.

feasibility of novel MRI techniques (13, 28–30) for placental perfusion and maternal adiposity. The study was blinded to pregnancy outcomes, but due to the nature of the study, the MRI acquisition protocol was continually updated over the course of the subject recruitment, particularly at the beginning of the study. The subjects underwent MRI studies temporally at 2 timepoints: 14 to 16 weeks gestational age (GA), and 19 to 24 weeks GA (Fig. 1A). Two Siemens 3T MRI scanners (Skyra and Prisma MAGNETOM; Siemens Healthineers, Erlangen, Germany) were used for the imaging experiments using a body matrix array and spine array coils. All subjects underwent MRI scans in a feet-first, supine position. The final

MRI acquisition protocol included a T2-weighted half-Fourier single-shot turbo spin-echo (T2-HASTE) sequence for placenta volume measurement (cm^3), a free-breathing 3D pseudo-continuous arterial spin labeling (pCASL) sequence (13, 28) to measure placenta perfusion, and a free-breathing multi-echo gradient echo sequence (29) to obtain maternal adiposity measures. Some subjects obtained only 1 MRI scan at 1 of the 2 time-points (n = 10), and the cases with severe imaging artifacts, potentially due to amniotic fluid and subject/uterine motion, were excluded from the analysis (n = 10), leading to different numbers of MRI data available for analyses. Figure 1B shows the flowchart for the inclusion of image analyses.

For each subject, a clinical fellow (B.L.), supervised by an experienced maternal-fetal medicine specialist (C.J., with 20 years of experience), confirmed the placental regions of interest (ROIs) placement on T2-HASTE, placenta blood flow (PBF; mL/100 g/min) and a fat fraction map (31) (0%-100%; a ratio of fat signal to the sum of the fat and water signals), blinded to the pregnancy outcome. The confirmed ROIs included placenta, subcutaneous and visceral fat areas, and whole-body and visceral areas. The maternal adiposity was assessed by the abdominal adiposity measures, such as subcutaneous fat area ratio (SFAR) and visceral fat area ratio (VFAR).

A diagram illustrating the image analysis for placental volume analysis is shown in Fig. 2. A placental region of interest (ROI, green outline in Fig. 2) was manually drawn in the axial, sagittal, and coronal planes, for each MRI slice in which the placenta was visible. Using OsiriX MD (Pixmeo Sarl, Bernex, Switzerland), a volumetric calculation was performed for the placental ROIs, revealing the total 3-D volume of the placenta.

A diagram illustrating the image analysis steps for the maternal adiposity is shown in Fig. 3. The maternal adiposity analysis was performed on an axial slice at each of the 5 lumbar vertebral levels by comparing to the subject's sagittal plane (Fig. 3A). Four regions of interest were measured: the
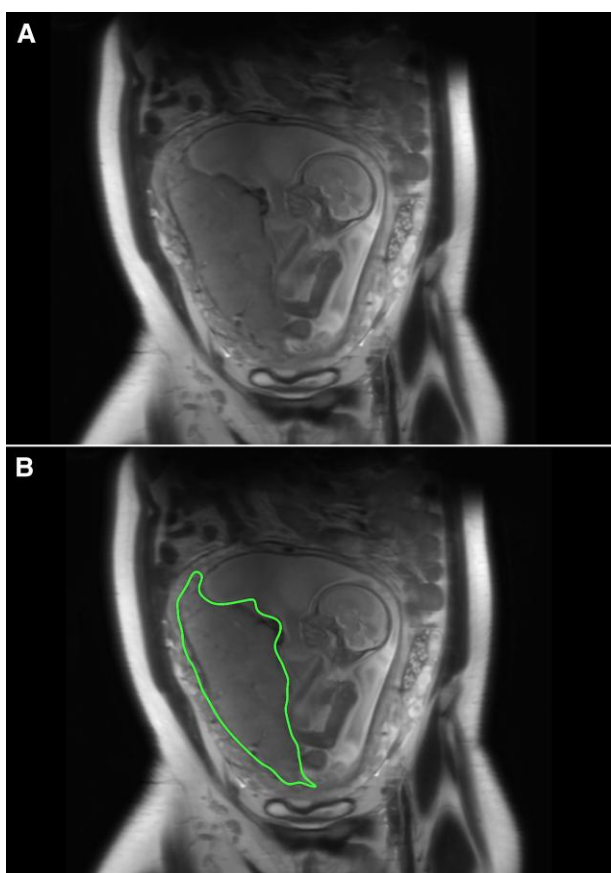

Figure 2. Placental volume. To determine placental volume, placental regions of interest were traced manually. The two images above are the same; the top image (A) shows an MRI slice in the coronal plane of the placenta and fetus; the bottom image (B) shows the placental region traced in green. This was repeated for all MRI slices in which the placenta was visible, for each the axial, coronal, and sagittal planes, allowing for the determination of placental volume.

subcutaneous fat area (Fig. 3B), total body area (Fig. 3C), visceral fat area (Fig. 3D), and total visceral area (Fig. 3E). For measurements of the total body area and total visceral area, the area taken up by the uterus was subtracted. Areas of interest were measured by segmenting a region of interest using a combination of manual selection and the Osirix Grow Region tool, with the area calculation performed by Osirix. SFARs were then created for each patient by dividing the subcutaneous fat area by the total body area, and then averaged over each of the 5 lumbar vertebral spine levels. VFARs were created for each patient by dividing the visceral fat area by the total visceral area, and then averaged over each of the 5 lumbar vertebral spine levels.

Statistical Analysis

A priori power calculations for arriving at the sample size (~200 subjects) for the prospective clinical study was based on the primary objective of developing and evaluating cutting-edge MRI technologies that enable safe and non-invasive assessment of placental structure and function in the context of placental dysfunction (13, 28). Subsequently for our preplanned secondary analysis of GDM as the outcome measure, we anticipated an incidence of 8% in Los Angeles consisting of 16 subjects in our recruitment cohort to subsequently develop GDM. Under this assumption, we predicted having adequate power (>99%) in our planned data analyses and multiple logistic regression analyses for GDM as the outcome with an expected AUC of 0.80 and margin of error of 0.13 at the confidence interval of 95%. The subjects with a history of preexisting diabetes mellitus, abortion (spontaneous or planned termination), and lost to follow-up or who withdrew from the study were not included in the analysis (Fig. 1B). Differences between the control group and GDM group were compared using a two-tailed t test. A P value less than or equal to 0.05 was considered significant. Simple and multiple logistic regression analyses were performed to evaluate different classification models as proof of concept, with the outcome variable being the development of GDM using either individual or a combination of MRI-based imaging features from placenta volume, placental perfusion, and maternal adiposity. Data imputation was not used to replace missing MRI-based imaging features. The logistic regression modeling was done a posteriori and cumulatively for all measurements at both MRI time points (14-16 weeks and 19-24 weeks), for 3 separate BMI categories: all (any BMI), nonobese (BMI < 25), and obese (BMI ≥ 25). We identified the optimal cutoff point for the prediction of GDM by maximizing Youden's index on receiver operator characteristic (ROC) curves. All the analyses were compared based on the area under the ROC curve (AUC). Sensitivity, specificity, positive predictive value (PPV), and negative predictive value (NPV) of the classification test (GDM vs control) were reported from the optimal cutoff point.

Results

Participant and Study Demographics

Of the 199 recruited women, a total of 186 subjects were analyzed for placental function and maternal adiposity (Fig. 1B). The partial inclusion of subjects in the analysis was due to the nature of technical limitations faced early on in the study while fulfilling the primary objective for the study enrollment
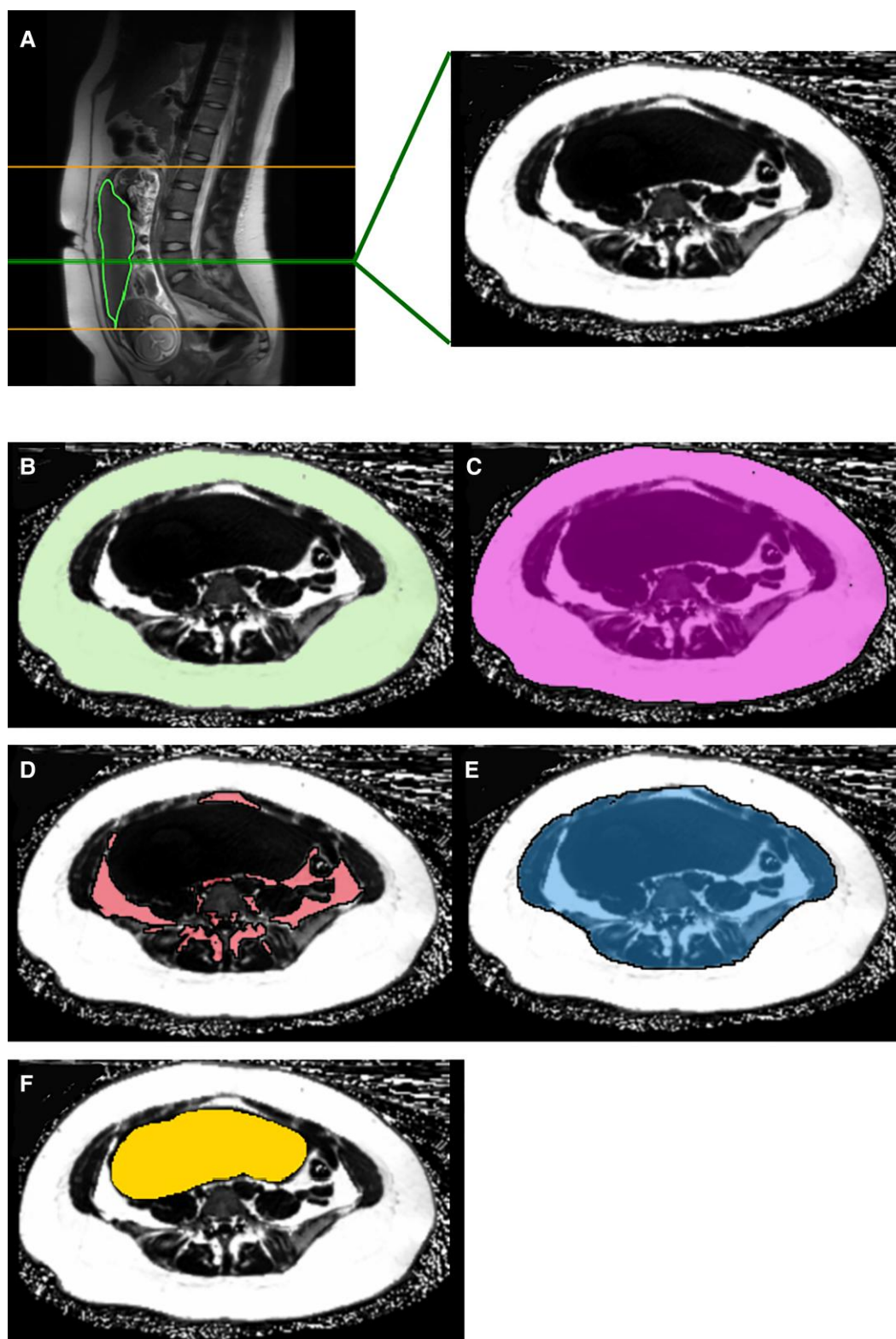
Figure 3. Maternal adiposity analysis. A) a sagittal plane MRI image (top left) of a representative subject showing the corresponding axial plane (top right) at lumbar vertebral level L5 (horizontal green line in the sagittal plane). B) The subcutaneous fat area of image A is highlighted in green. C) The total body area of image A is highlighted in pink. D) The visceral fat area of image A is highlighted in red. E) The total visceral area of image A is highlighted in blue. F) The uterus in image A is highlighted in yellow.

(13, 28–30), and not due to a loss of follow-up. 165 women (88.7%) did not develop gestational diabetes (GDM), forming our control group. 21 women developed GDM (11.3%), forming our GDM group. Of all the analyzed subjects, 176 underwent an MRI scan at the first timepoint of 14 to 16 weeks and 166 underwent an MRI scan at the second timepoint of 19 to 24 weeks. Maternal characteristics are shown in Table 1. There were no significant differences in maternal

Table 1. Patient characteristics

	Control group (n = 165)	GDM group (n = 21)	*P* value
Mean age at consent (years ± SD)	24.4 ± 4.6	24.9 ± 4.8	0.64
Gestational age at first MRI (weeks)	15.7 ± 1.0	15.9 ± 1.1	0.29
Gestational age at second MRI (weeks)	20.8 ± 1.2	20.8 ± 1.3	0.99
Pre-pregnancy BMI (kg/m^2)	24.4 ± 4.6	24.9 ± 4.8	0.61
Fetal Sex	Male: 88 (53.3%) Female: 77 (46.7%)	Male: 12 (57%) Female: 9 (43%)	
Multigravida	91 (55.1%)	7 (33%)	
Multiparous	18 (10.9%)	3 (14%)	
Prior history of GDM	0 (0%)	6 (28.6%)	
Developed preeclampsia in this pregnancy	15 (9%)	1 (4.8%)	
Prior history of preeclampsia	7 (4.2%)	1 (4.8%)	
Race/ethnicity (n, % of total control group)			
White, non-Hispanic	78 (47.2%)	8 (38%)	
Hispanic	33 (20%)	4 (19%)	
Asian	42 (25.4%)	9 (43%)	
Black or African American	11 (6.7%)	0 (0%)	
American Indian or Alaska Native	1 (0.6%)	0 (0%)	

age at consent, gestational age at the first MRI time point, gestational age at the second MRI time point, or pre-pregnancy BMI between the GDM and control groups.

Placental Function

At the first timepoint of 14 to 16 weeks, there were 176 placental MRI scans. Of those, 156 were from control subjects, and 20 were from GDM subjects. At the second timepoint, there were 166 placental MRI scans; of those, 146 were from control subjects and 20 were from GDM subjects.

Placental volume

Placental volumes (Table 2, Fig. 4) measured at the first MRI timepoint did not show any difference between the control and GDM groups but showed a trend towards larger mean placental volumes in the GDM group (control: 137.1 cm^3 vs GDM: 152.1 cm^3, *P* = 0.19). At the second MRI time point, mean placental volume was significantly greater in the GDM group when compared to the control group (control: 255.7 cm^3 vs GDM: 301.0 cm^3; *P* = 0.01). The percent change in placental volume per week between the first and second MRI time point, as an overall average per individual subject, was significantly greater in the GDM group among all BMI categories (Control: 563.5%/week vs GDM: 656.0%/week, *P* = 0.01). ROC curves generated for placental volume at the first and second timepoints for the outcome of GDM showed an area under the curve of 0.57 and 0.66, respectively (Supplemental Fig. S1) (32).

Placental perfusion

Placental perfusion was measured by the following parameters: PBF, high PBF (hPBF), and arterial transit time (ATT), as shown in Table 3 and Fig. 4.

While no significant differences emerged, at the first MRI time point of 14 to 16 weeks, PBF trended lower in the GDM group as compared to the control group, among all BMI categories. This trend continued to be seen when separated into an obese cohort and nonobese cohort. Similarly, hPBF trended lower in the GDM group as compared with the control group, among all BMI categories, as well as when separated into an obese cohort and nonobese cohort. ATT trended higher in the GDM group as compared with the control group among all BMI categories, as well as when separated into an obese cohort and nonobese cohort. At the first MRI time point of 14 to 16 weeks GA, ROC curves generated for PBF show an AUC of 0.54, 0.61, and 0.52 for all BMI categories combined, the obese cohort, and the nonobese cohort, respectively (Supplemental Fig. S2) (32). ROC curves generated for hPBF show an AUC of 0.61, 0.71, and 0.52, for all combined BMI categories, the obese cohort, and the nonobese cohort, respectively (Supplemental Fig. S3) (32).

At the second MRI time point of 19 to 24 weeks (Table 3), PBF was significantly reduced in the obese GDM cohort compared with the obese control cohort (control: 78.59 mL/100 g/min, vs GDM: 63.68 mL/100 g/min, *P* = 0.04). The other measured parameters did not achieve statistical significance between GDM vs controls but continued to show lower trends in the GDM group as compared with the control group, among all BMI categories, as well as when separated into an obese cohort and nonobese cohort. The hPBF trended lower in the GDM group as compared to the control group, among all BMI categories when combined, as well as when separated into an obese cohort and nonobese cohort. ATT trended higher in the GDM group as compared with the control group, when separated into a nonobese cohort. At the second MRI time point of 19 to 24 weeks GA, ROC curves generated for PBF showed an AUC of 0.59, 0.70, and 0.57 for all combined BMI categories, the obese cohort, and the nonobese cohort, respectively (Supplemental Fig. S4) (32). ROC curves generated for hPBF showed an AUC of 0.57, 0.65, and 0.53 for all combined BMI categories, the obese cohort, and the nonobese cohort, respectively (Supplemental Fig. S5) (32).

Table 2. Placental volumes (in cm^3) at the first (14-16 weeks) and second (19-24 weeks) MRI time points for the control group and gestational diabetes (GDM) group

	All BMI categories			Obese cohort			Nonobese cohort		
	Control	GDM	P value	Control	GDM	P value	Control	GDM	P value
Volume at first MRI [cm^3] (n)	137.1 ± 46.5 (155)	152.1 ± 58.2 (20)	0.19	143.5 ± 38.7 (54)	151.7 ± 71.5 (9)	0.61	133.7 ± 50.0 (101)	152.4 ± 48.5 (11)	0.24
Volume at second MRI [cm^3] (n)	255.7 ± 72.2 (146)	301.0 ± 84.9 (20)	0.01	267.9 ± 77.9 (50)	322.5 ± 105.7 (10)	0.06	229.4 ± 68.3 (96)	279.4 ± 55.0 (10)	0.18
% Change between first and second MRI [%/week] (n)	563.5 ± 140.6 (144)	656.0 ± 224.0 (19)	0.01	548.6 ± 148.4 (49)	665.5 ± 255.6 (9)	0.06	573.3 ± 137.1 (91)	599.4 ± 193.2 (14)	0.56

Statistical analysis done via two-tailed t test. First MRI time point was 14-16 weeks; second MRI time point was 19-24 weeks. Subjects in the obese cohort had a BMI ≥ 25.0. Subjects in the nonobese cohort had a BMI < 25.0.
Abbreviations: BMI, body mass index (kg/m^2); GDM, gestational diabetes.

Maternal Adiposity

At the first timepoint of 14 to 16 weeks, there were 109 with MRI sequences for analysis of maternal adiposity; of these, 13 were from subjects who developed GDM, and 96 were from subjects who did not develop GDM. At the second timepoint of 19 to 24 weeks, there were 109 with MRI sequences for analysis of maternal adiposity; of these, 19 were from subjects who developed GDM, and 90 were from subjects who did not develop GDM. Results of maternal adiposity are shown in Table 4.

Subcutaneous adiposity

At the first timepoint of 14 to 16 weeks (Table 4), the mean SFAR in the control group was 38.8% (SD 11.1%, n = 96) vs 39.8% (SD 10.5%, n = 13) in women who developed GDM. At the second timepoint of 19-24 weeks, the mean SFAR in the control group was 39.8% (SD 9.4%, n = 90) vs 40.4% (SD 11.0%, n = 19) in women who developed GDM. There was no significant difference in SFAR between the control group and GDM group at either the first or second timepoint, with $P = 0.76$ and $P = 0.81$, respectively, as measured by two-tailed t test. There was no significant difference in SFAR between the control group and GDM group when separated into obese and nonobese cohorts. ROC curves generated for SFAR at the first and second MRI timepoints show an AUC of 0.51 and 0.50, respectively (Fig. 5A and 5B).

Visceral adiposity

At the first timepoint of 14-16 weeks, the mean VFAR in the control group was 19.2% (SD 6.7%, n = 96), and the mean VFAR in women who developed GDM was 26.9% (SD 5.0%, n = 13). At the second timepoint of 19 to 24 weeks, the mean VFAR in the control group was 17.9% (SD 5.8%, n = 89), and the mean VFAR in women who developed GDM was 24.1% (SD 5.6%, n = 19). The VFAR was significantly higher in the GDM group, as compared with the control group, at both the first and second timepoints ($P < 0.001$ for both, Table 4, Fig. 6) as measured by two-tailed t test. When separated into an obese cohort and nonobese cohort, VFAR values continue to be significantly increased in the GDM groups, as compared with the respective control groups. The exception is the obese cohort at the first MRI time point, where values for VFAR trended lower in the GDM group but did not reach statistical significance ($P = 0.06$). ROC curves generated for VFAR at the first and second timepoints for all subjects showed an AUC of 0.82 and 0.77, respectively (Fig. 5C and 5D).

Relationship of Maternal Adiposity to BMI

At the first MRI time point of 14 to 16 weeks GA, SFAR and VFAR were significantly higher in the overweight/obese cohort of the control group, compared with the nonobese cohort of the control group, as measured by two-tailed t test ($P < 0.001$ for both). For the GDM group at the first MRI, SFAR and VFAR values trended higher, but did not reach statistical significance, for the overweight/obese cohort within the GDM group as compared with the nonobese cohort within the GDM group.

At the second MRI time point of 19 to 24 weeks, the overweight/obese cohort within the control group had significantly higher SFAR and VFAR values as compared with the nonobese counterparts ($P < 0.001$ for both). Similarly, the overweight/obese cohort within the GDM group had
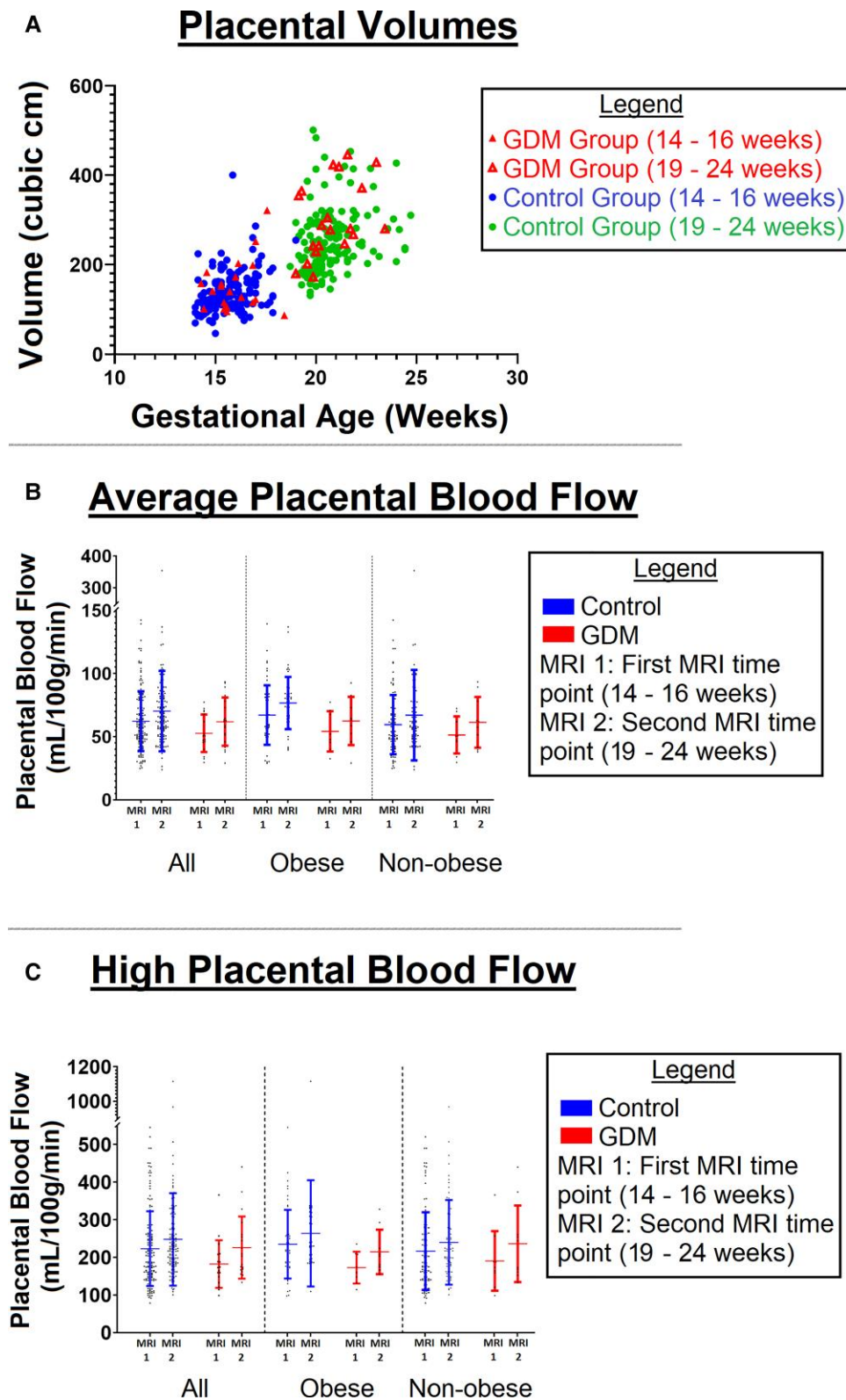
Figure 4. Placental function analysis. A) Scatter plots showing placental volumes (in cubic centimeters) plotted by gestational age (GA). Control group volumes are represented at the first MRI time point of 14-16 weeks GA (blue dots) and second MRI time point of 19-24 weeks GA (green dots). The gestational diabetes (GDM) group is represented by red triangles, at the first (filled red triangle) and second (open red triangle) MRI time point. B) Mean and standard deviations for values of regions of average placental blood flow (PBF, in mL/100 g/min) in all subjects, overweight/obese subjects, and nonobese subjects. Blue bars represent the control group; red bars represent the GDM group. The graph shows PBF at the first and second MRI time points (MRI 1: 14-16 weeks GA, and MRI 2: 19-24 weeks GA, respectively). The PBF values trended lower in the gestational diabetes (GDM) group for every comparison between the respective control group values. C) Mean and standard deviations for values of regions of high placental blood flow (hPBF, in mL/100 g/min) in all subjects, overweight/obese subjects, and non-obese subjects. Blue bars represent the control group; red bars represent the GDM group. The graph shows hPBF at the first and second MRI time points (MRI 1: 14-16 weeks GA, and MRI 2: 19-24 weeks GA, respectively). The hPBF values trended lower in the gestational diabetes (GDM) group for every comparison between the respective control group values.

Table 3. Comparison of markers of placental perfusion by BMI category, at first and second MRI timepoints

|		All BMI Categories			Obese Cohort			Non-obese Cohort		
		Control	GDM	P value	Control	GDM	P value	Control	GDM	P value
First MRI time point (14-16 weeks GA)	PBF (n)	64.23 ± 21.9 (156)	56.59 ± 13.1 (17)	0.16	70.35 ± 22.8 (55)	59.12 ± 15.2 (8)	0.18	60.89 ± 20.8 (101)	54.34 ± 11.4 (9)	0.35
	hPBF (n)	228.72 ± 106.0 (156)	180.69 ± 68.6 (17)	0.07	242.14 ± 101.8 (55)	171.58 ± 45.7 (8)	0.06	221.41 ± 108.0 (101)	188.79 ± 86.2 (9)	0.38
	ATT (n)	1391.80 ± 98.1 (156)	1430.70 ± 119.1 (17)	0.13	1409.65 ± 103.1 (55)	1436.48 ± 120.6 (8)	0.50	1382.08 ± 94.3 (101)	1425.56 ± 124.8 (9)	0.20
Second MRI time point (19-24 weeks GA)	PBF (n)	72.71 ± 32.6 (145)	62.55 ± 16.5 (19)	0.20	78.59 ± 19.8 (49)	63.68 ± 16.7 (9)	0.04	69.71 ± 38.6 (96)	61.53 ± 17.2 (10)	0.51
	hPBF (n)	255.3 ± 132 (145)	227.30 ± 87.7 (19)	0.38	272.49 ± 160.1 (49)	214.75 ± 60.1 (9)	0.30	245.38 ± 114.0 (96)	238.61 ± 108.9 (10)	0.86
	ATT (n)	1377 ± 90.5 (145)	1376.92 ± 218.9 (19)	>0.99	1384.96 ± 82.2 (49)	1320.40 ± 309.0 (9)	0.21	1372.87 ± 94.2 (96)	1427.78 ± 69.6 (10)	0.08

First MRI time point was 14-16 weeks; second MRI time point was 19-24 weeks. Subjects in the obese cohort had a BMI ≥ 25.0. Subjects in the non-obese cohort had a BMI <25.0.
Abbreviations: ATT, arterial transit time (ms); BMI, body mass index (kg/m²); GA, gestational; age; GDM, gestational diabetes; hPBF, high placental blood flow (mL/100 g/min); PBF, average placental blood flow (mL/100 g/min).

Table 4. Comparison of subcutaneous fat area ratio (SFAR) and visceral fat area ratio (VFAR) by BMI category, at first and second MRI timepoints

		All BMI Categories			Obese Cohort			Non-obese Cohort		
		Control	GDM	P value	Control	GDM	P value	Control	GDM	P value
First MRI Time point (14-16 weeks GA)	SFAR [Mean % ± SD%] (n)	38.8 ± 11.1 (96)	39.8 ± 10.5 (13)	0.76	45.6 ± 9.6 (36)	43.9 ± 10 (6)	0.69	34.8 ± 10.0 (60)	36.4 ± 9.8 (7)	0.68
	VFAR [Mean % ± SD%] (n)	19.3 ± 6.7 (96)	26.9 ± 5.0 (13)	<0.001	23.3 ± 6.8 (36)	28.9 ± 5.4 (6)	0.06	16.7 ± 5.3 (60)	25.1 ± 4.1 (7)	<0.001
	BMI [kg/m²] (n)	24.6 ± 4.4 (96)	25.1 ± 4.7 (13)	0.66	29.5 ± 4.7 (36)	29.0 ± 4.0 (6)	0.81	21.5 ± 2.0 (60)	21.9 ± 1.9 (7)	0.66
	Age [years] (n)	33.8 ± 3.7 (95)	34.2 ± 4.1 (13)	0.71	34.6 ± 4.1 (35)	35.3 ± 4.5 (6)	0.69	33.3 ± 3.4 (60)	33.3 ± 3.8 (7)	0.96
Second MRI Time point (19-24 weeks GA)	SFAR [Mean % ± SD%] (n)	39.8 ± 9.4 (90)	40.4 ± 11 (19)	0.81	45.9 ± 7.8 (36)	47.1 ± 8.2 (10)	0.65	35.8 ± 8.2 (54)	32.3 ± 8.3 (9)	0.34
	VFAR [Mean % ± SD%] (n)	17.9 ± 5.8 (89)	24.1 ± 5.6 (19)	<0.001	22.0 ± 5.3 (35)	27.0 ± 5.6 (10)	0.01	15.3 ± 4.4 (54)	20.9 ± 3.5 (9)	<0.001
	BMI [kg/m²] (n)	24.7 ± 5.1 (90)	25.4 ± 4.8 (19)	0.55	29.4 ± 4.6 (36)	29.0 ± 3.6 (10)	0.79	21.5 ± 2.1 (54)	21.5 ± 1.8 (9)	0.79
	Age [years] (n)	33.7 ± 3.8 (89)	34.3 ± 3.6 (19)	0.53	34.2 ± 4.4 (36)	35.5 ± 3.4 (10)	0.37	33.4 ± 3.3 (54)	32.9 ± 3.6 (9)	0.37

Subjects in the obese cohort had a BMI ≥ 25.0. Subjects in the non-obese cohort had a BMI <25.0.
Abbreviations: GDM = gestational diabetes; BMI = body mass index (kg/m²); SFAR = subcutaneous fat area ratio; VFAR = visceral fat area ratio. First MRI time point was 14-16 weeks; second MRI time point was 19-24 weeks.

Subcutaneous Fat Area Ratios (SFAR)
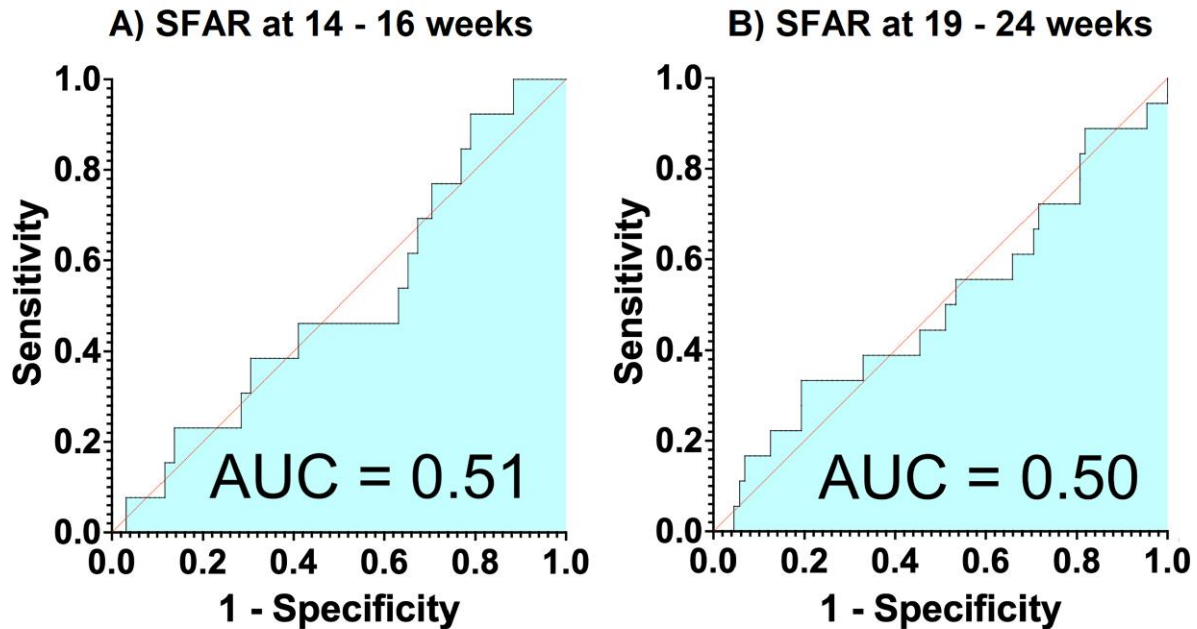
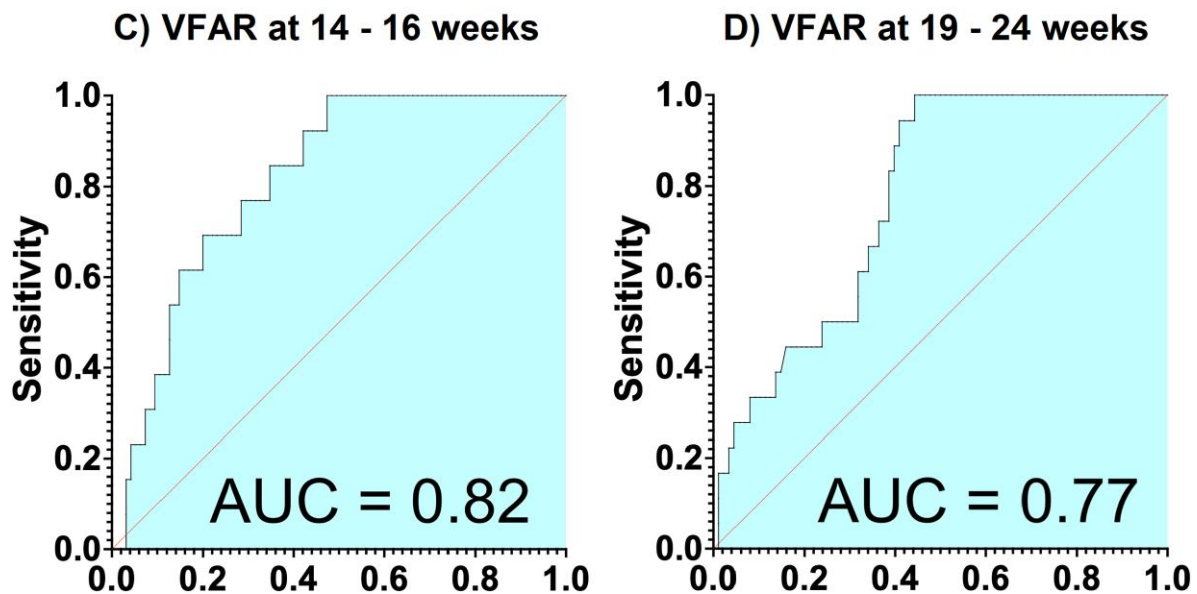# Visceral Fat Area Ratios (VFAR)

Figure 5. Receiver operating characteristic curves for subcutaneous fat area ratio (SFAR) and visceral fat area ratio (VFAR) analysis at 14-16 weeks gestational age (GA) and at 19-24 weeks GA, for the outcome of gestational diabetes. Areas under the curve (AUC) for SFAR were 0.51 at 14-16 weeks GA (A, top left), and 0.50 at 19-24 weeks GA (B, top right). AUCs for VFAR were 0.82 at 14-16 weeks GA (C, bottom left), and 0.77 at 19-24 weeks GA (D, bottom right).
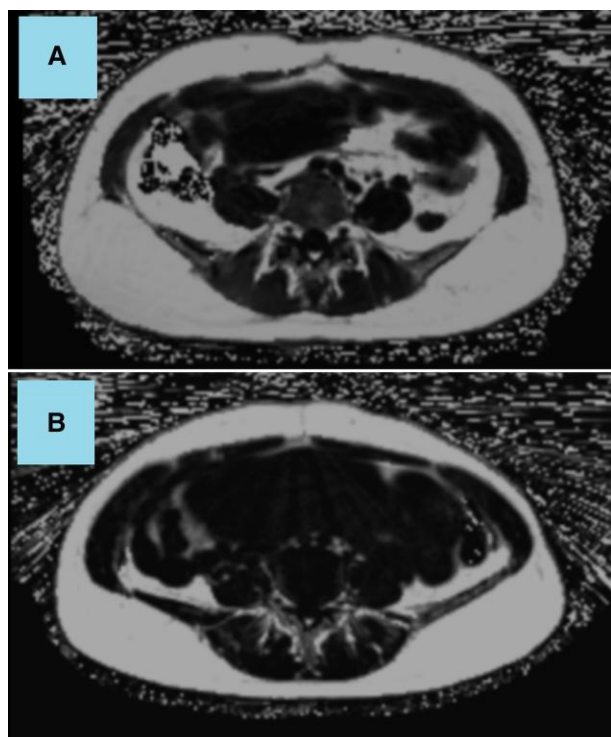
Figure 6. MRI images. Comparison of representative MRI images of two different subjects in the axial plane. A patient with gestational diabetes (GDM) is shown in the top image (A), versus a patient who did not develop GDM in the bottom image (B), at similar axial MRI level. Both patients had a pre-pregnancy BMI in the Normal weight, yet visceral adiposity is visibly higher in the GDM patient (A).

significantly higher SFAR and VFAR values as compared with the nonobese cohort within the GDM group ($P = 0.002$ and $P = 0.01$, respectively).

Relationship of Prepregnancy BMI and Race to the Development of GDM

A simple logistic regression examining the relationship of pre-pregnancy BMI to the development of GDM revealed a ROC curve (Supplemental Fig. S6) (32) with an AUC of 0.53. We also compared values of placental perfusion and adiposity between subjects who self-identified as White and non-Hispanic race, vs those who identified as Black or African American race and found that there was no significant difference between any parameters of the placental function (volume or perfusion values) and maternal adiposity (both subcutaneous and visceral) between the two different race categories.

Multiple Logistic Regression Analyses

Combining placental blood flow and high blood flow with visceral adiposity at the first MRI time point (Fig. 7), the AUC for all cohorts was 0.83; for the obese cohort was 0.84; and for the nonobese cohort was 0.90. At the second MRI time point (Fig. 7), the AUC for all cohorts was 0.81; for the obese cohort was 0.82; and for the nonobese cohort was 0.83. PPV for GDM using the combination of placenta perfusion and visceral adiposity was 0.78, and NPV was 0.83 at 14 to 16 weeks with a sensitivity and specificity of 0.85 and of 0.77, while PPV and NPV were 0.73 and 0.86 at 19 to 24 weeks with a sensitivity and specificity of 0.89 and 0.67.

Summary of Results

A combination of MRI features that included hPBF, PBF, and VFAR together provided a more robust association and predictability of GDM than any feature alone, and was far better than that seen with pre-pregnancy BMI alone. In addition, VFAR and placental volume were increased in GDM vs controls, particularly in the nonobese cohort, while placental perfusion trended lower in GDM when compared to controls.

Discussion

Our study is the first to combine a longitudinal MRI assessment of placental function as measured by placental volume and perfusion with maternal adiposity, in early gestation, in the context of gestational diabetes. We provide potential values for assessing placenta perfusion and visceral adiposity in pregnant women who do or do not develop GDM, and we demonstrate the possible utility of MRI in early gestation for predicting GDM. We found a nonsignificant trend for decreased placental perfusion in patients who developed GDM, when compared with those who did not develop GDM. While our results were not statistically significant, there was a consistent trend in the reduction of placental function across all parameters of placental perfusion even with a small cohort of patients who developed GDM.

Our multiple logistic regression analyses showed an AUC of 0.83 using a combination of visceral adiposity and placental perfusion at 14 to 16 weeks. Based on power analysis, 13 GDM and 96 control subjects (the minimum number of subjects across the analytic samples) had > 90% power to demonstrate the association between MRI-based imaging features and GDM with a true AUC of 0.80 and a two-sided significance level of 0.05. The sensitivity and specificity at the optimal cutoff point respectively were 0.85 and 0.77 at 14 to 16 weeks and 0.89 and 0.67 at 19 to 24 weeks, which outperformed other imaging studies that have attempted to evaluate maternal adiposity in association with GDM, including ultrasound measurements of adiposity (21, 23–25). In particular, Nassr et al showed that ultrasound measurements of visceral fat and parietal fat for early screening of GDM had a ROC curve with an AUC of 0.69 and 0.72 respectively (23). Furthermore, in our present study, high AUCs were seen in the nonobese cohort (0.90 at 14-16 weeks and 0.83 at 19-24 weeks), which is important, as these patients may be overlooked for potentially developing GDM if BMI is used as a high risk indicator for screening.

Gur et al found that visceral fat thickness was a good predictor of GDM, with a ROC AUC of 0.66 for maximum visceral fat thickness (24). Compared with other imaging studies, our present study shows a greater AUC for the development of GDM using MRI measurements of maternal adiposity. Ultrasonography can only measure adiposity to a limited depth, while our MRI measurements provide a quantitative and volumetric measurement of adiposity for the entire body area.

Another biomarker commonly used as a risk factor for developing GDM is BMI. We found that subcutaneous and visceral adiposity significantly increased with increasing BMI, as predicted. However, we also showed that prepregnancy BMI was only a predictor of adiposity as a whole and could not differentiate between subcutaneous and visceral adiposity. In addition, through a simple logistic regression analysis, we found that prepregnancy BMI by itself was not a
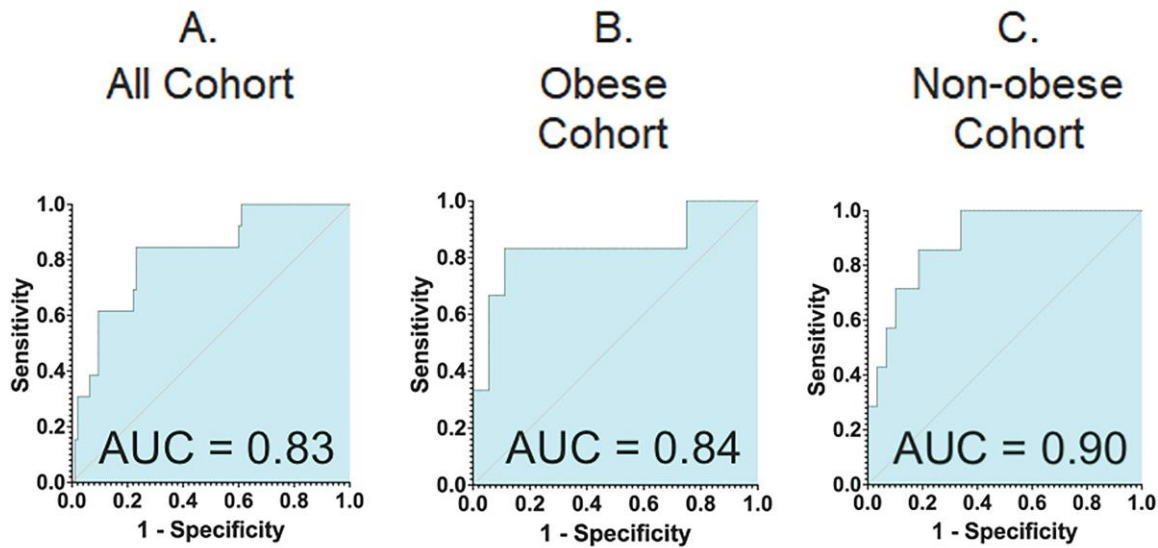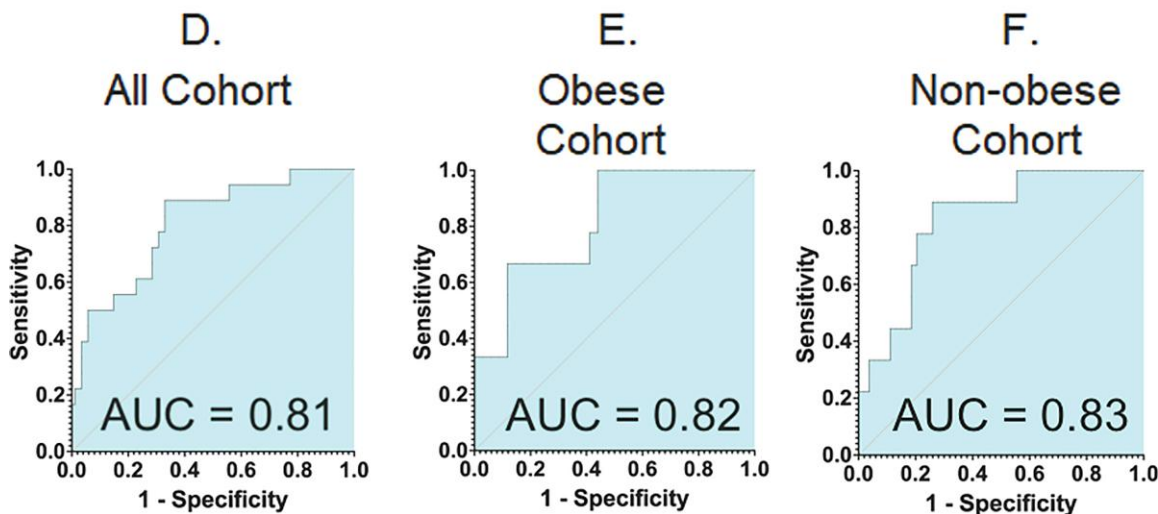
Figure 7. Multiple logistic regression analysis for the outcome of gestational diabetes (GDM) at 14-16 weeks gestational age (GA), and 19-24 weeks GA. Receiver operating characteristic curves of the multiple logistic regression analysis using VFAR, high placental blood flow, and placental blood flow for the outcome of GDM. The top row depicts the analysis at the first MRI time point of 14-16 weeks GA. "All cohort" (A, top left) includes subjects of any BMI. "Obese cohort" (B, top middle) includes overweight and obese subjects. "Non-obese cohort" (C, top right) includes underweight and Normal weight subjects. The area under the curves are A. 0.83, B. 0.84, and C. 0.90, respectively. The bottom row depicts the analysis at the second MRI time point of 19-24 weeks GA. "All cohort" (A, bottom left) includes subjects of any BMI. "Obese cohort" (B, bottom middle) includes overweight and obese subjects. "Non-obese cohort" (C, bottom right) includes underweight and Normal weight subjects. The area under the curves are A. 0.81, B. 0.82, and C. 0.83, respectively.

useful predictor in the subsequent development of GDM. Thus, maternal adiposity as measured by MRI, in order to show its distribution throughout the body, particularly visceral adiposity, is more important for the prediction of

GDM, even if such analysis was undertaken more as a proof of concept, requiring further validation in the future.

An earlier study by Takahashi et al in 2014 (26) measured SFAR and VFAR at 15 to 18 weeks GA in women with a

prepregnancy BMI greater than 25. Their study had comparable SFAR values, but higher VFAR values than our study. This may be because Takahashi's study excluded nonobese patients, while our study included underweight, normal weight, and obese patients. Takahashi's study also included MRI scans at levels above and below those employed in our study, so it is difficult to make a valid comparison between the two studies.

We considered certain confounding factors during our analysis. BMI is a factor that may have confounded our results for maternal adiposity. To evaluate this, we compared differences in adiposity and placental function separately in the control and GDM groups, by separating the two groups into an obese and nonobese cohort. We found that the trends in larger placental volumes and reduction in placental perfusions remained consistent even when taking BMI into account (Supplemental Table S1) (32). The development of preeclampsia may have confounded our results for placental function. We compared our results after excluding pregnant women who had a history of preeclampsia and those who developed preeclampsia during the study. We confirmed that excluding these subjects did not affect our findings, and the adiposity and placental function measurements had similar predictive capabilities regardless of the status of pre-eclampsia (Supplemental Tables S1-S3; Supplemental Figs. S7 and S8) (32). It also must be considered that the changes in adiposity and placental function may be an early contributing factor to the development of GDM, as opposed to being a result of GDM itself.

Our study has strengths in its prospective design. In addition, our control group is representative of the different types of pregnant women coming from the community without preselection for clinical high-risk factors; they were not chosen due to any past medical history or prior diagnosis of gestational diabetes. Our study applies MRI to the development of GDM, showing the feasibility of this imaging modality in early-gestation to improve our understanding and opens the possibility of entertaining prediction of the subsequent development of GDM. While currently, the utilization of MRI would be less cost-effective as an early-gestation screening tool for GDM, noninvasive imaging methods can further our understanding of how maternal and placental changes in early gestation occur in the context of GDM. Epigenetic studies have shown that combinations of biomarkers to predict adverse pregnancy outcomes, including GDM, may be possible. A subset of patients who demonstrate association with certain early circulating biomarkers may additionally benefit from further noninvasive MRI evaluation after the initial screening (19, 20).

Our study contained a few limitations. A practical limitation of our study is a preplanned secondary analysis of MRI data obtained as part of the Human Placental Project, which required developing and testing the feasibility of novel MRI techniques (13, 28–30). Thus, we have several subjects, particularly when enrolled during the early phase of the clinical trial, who do not have maternal adiposity data due to certain technical limitations, despite having undertaken MRI scans while being blinded to the pregnancy outcome. Furthermore, not every subject underwent 2 MRI scans, despite continuing in the study and not being lost to study follow-up. Despite this limitation, we have analyzed the data separately with only patients who have complete sets of MRI data (ie, subjects with 2 MRI scans with both adiposity and perfusion measures) and

found that the trending of decreased placental perfusion and significantly increased visceral adiposity persisted. Another limitation of our study is the small size of the GDM group. Of the 186 analyzed subjects, 21 women (11.3%) developed GDM. Even with a small group of GDM patients, our results show a consistent difference in measurements of adiposity and placental function between the GDM and control patients. The number of individuals who developed GDM is higher than average and may reflect the location of our antenatal obstetrics clinics in high-risk areas of Los Angeles. The final results of our study are also not stratified by race or socioeconomic factors, both of which may modify the risk for development of gestational diabetes (33). However, we did assess subcutaneous and visceral adiposity in the control group between different self-reported ethnic groups (Supplemental Table S3) (32), and also stratified by sex of the fetus (Supplemental Table S4) (32). Future studies in a larger cohort including both control and GDM groups are warranted.

Conclusion

We have shown that placental perfusion and maternal visceral adiposity are significantly associated with GDM and present the possibility of being predictive of the subsequent development of GDM. These findings correlate with our understanding of the association between visceral adiposity and placental perfusion during early pregnancy in the setting of GDM. MRI measurements could perhaps serve more as an adjunct to the subset of GDM subjects who demonstrate an association with circulating biomarkers characteristic of GDM. Few studies have explored the noninvasive measurement of maternal adiposity and placental function using MRI in early gestation in predicting GDM; this study provides a proof of concept and broadens the potential for further studies exploring the utility of MRI in the prediction of GDM and potentially other adverse pregnancy outcomes. Further studies exploring the utility of early-gestation MRI may help strengthen the role of MRI in predicting the subsequent development of GDM.

Disclosures

The authors have no disclosures and have no potential conflicts of interest.

Data Availability

Some or all datasets generated during and/or analyzed during the current study are not publicly available but are available from the corresponding author on reasonable request.

References

1. Deputy NP, Kim SY, Conrey EJ, Bullard KM. Prevalence and changes in preexisting diabetes and gestational diabetes among women who had a live birth—United States, 2012-2016. *MMWR Morb Mortal Wkly Rep*. 2018;67(43):1201-1207.
2. Bardenheier BH IG, Gilboa SM. Trends in gestational diabetes among hospital deliveries in 19 U.S. States, 2000–2010. *Am J Prev Med*. 2015;49(1):12-19.

3. Bellamy L, Casas JP, Hingorani AD, Williams D. Type 2 diabetes mellitus after gestational diabetes: a systematic review and meta-analysis. *Lancet*. 2009;373(9677):1773-1779.

4. Tobias DK, Stuart JJ, Li S, *et al*. Association of history of gestational diabetes with long-term cardiovascular disease risk in a large prospective cohort of US women. *JAMA Intern Med*. 2017;177(12):1735-1742.

5. Kc K, Shakya S, Zhang H. Gestational diabetes mellitus and macrosomia: a literature review. *Ann Nutr Metab*. 2015;66(Suppl 2):14-20.

6. Hedderson MM, Ferrara A, Sacks DA. Gestational diabetes mellitus and lesser degrees of pregnancy hyperglycemia: association with increased risk of spontaneous preterm birth. *Obstet Gynecol*. 2003;102(4):850-856.

7. Lazer S, Biale Y, Mazor M, Lewenthal H, Insler V. Complications associated with the macrosomic fetus. *J Reprod Med*. 1986;31(6):501-505.

8. Lowe WL Jr, Lowe LP, Kuang A, *et al*. Maternal glucose levels during pregnancy and childhood adiposity in the hyperglycemia and adverse pregnancy outcome follow-up study. *Diabetologia*. 2019;62(4):598-610.

9. Mandl M, Haas J, Bischof P, Nöhammer G, Desoye G. Serum-dependent effects of IGF-I and insulin on proliferation and invasion of human first trimester trophoblast cell models. *Histochem Cell Biol*. 2002;117(5):391-399.

10. Vambergue A, Fajardy I. Consequences of gestational and pregestational diabetes on placental function and birth weight. *World J Diabetes*. 2011;2(11):196-203.

11. Palaiologou E, Etter O, Goggin P, *et al*. Human placental villi contain stromal macrovesicles associated with networks of stellate cells. *J Anat*. 2020;236(1):132-141.

12. Savvidou MD, Syngelaki A, Balakitsas N, Panaiotova E, Nicolaides KH. First-trimester uterine artery Doppler examination in pregnancies complicated by gestational diabetes mellitus with or without pre-eclampsia. *Ultrasound Obstet Gynecol*. 2013;42(5):525-529. .

13. Liu D, Shao X, Danyalov A, *et al*. Human placenta blood flow during early gestation with pseudocontinuous arterial spin labeling MRI. *J Magn Reson Imaging*. 2020;51(4):1247-1257.

14. ACOG Practice bulletin no. 190: gestational diabetes mellitus. *Obstet Gynecol*. 2018;131(2):e49-e64.

15. Greene MF. Drawing the line on glycemia in pregnancy. *N Engl J Med* 2022;387(7):652-654.

16. Crowther CA, Samuel D, McCowan LME, *et al*. Lower versus higher glycemic criteria for diagnosis of gestational diabetes. *N Engl J Med*. 2022;387(7):587-598.

17. Harper LM, Jauk V, Longo S, Biggio JR, Szychowski JM, Tita AT. Early gestational diabetes screening in obese women: a randomized controlled trial. *Am J Obstet Gynecol*. 2020;222(5):495.e1-495.e8.

18. Huhn EA, Rossi SW, Hoesli I, Gobl CS. Controversies in screening and diagnostic criteria for gestational diabetes in early and late pregnancy. *Front Endocrinol (Lausanne)*. 2018;9:696.

19. Del Vecchio G, Li Q, Li W, *et al*. Cell-free DNA methylation and transcriptomic signature prediction of pregnancies with adverse outcomes. *Epigenetics*. 2021;16(6):642-661.

20. Thamotharan S, Ghosh S, James-Allan L, Lei MYY, Janzen C, Devaskar SU. Circulating extracellular vesicles exhibit a differential miRNA profile in gestational diabetes mellitus pregnancies. *PLoS One*. 2022;17(5):e0267564.

21. AdS BJ R, Matos S, Kretzer DC, Schöffel AC, Goldani MZ. Maternal visceral adipose tissue during the first half of pregnancy predicts gestational diabetes at the time of delivery—a cohort study. *PLoS One*. 2020;15(4):e0232155.

22. Rojas-Rodriguez R LL, Bellve KD, Min SY, Pires J, Leung K. Human adipose tissue expansion in pregnancy is impaired in gestational diabetes mellitus. *Diabetologia*. 2015;58(9):2106-2114.

23. Nassr AA, Shazly SA, Trinidad MC, El-Nashar SA, Marroquin AM, Brost BC. 134. Utility of ultrasound measurement of maternal visceral and parietal fat for prediction of gestational diabetes. *Am J Obstet Gynecol*. 2016;214(1):S90-S91. https://doi.org/10.1016/j.ajog.2015.10.170

24. Gur EB IO, Turan GA. Ultrasonographic visceral fat thickness in the first trimester can predict metabolic syndrome and gestational diabetes mellitus. *Endocrine*. 2014;47(2):478-484.

25. Martin AM, Berger H, Nisenbaum R, *et al*. Abdominal visceral adiposity in the first trimester predicts glucose intolerance in later pregnancy. *Diabetes Care*. 2009;32(7):1308-1310.

26. Takahashi K, Ohkuchi A, Furukawa R, Matsubara S, Suzuki M. Establishing measurements of subcutaneous and visceral fat area ratio in the early second trimester by magnetic resonance imaging in obese pregnant women. *J Obstet Gynaecol Res*. 2014;40(5):1304-1307.

27. Guttmacher AE, Maddox YT, Spong CY. The human placenta project: placental structure, development, and function in real time. *Placenta*. 2014;35(5):303-304.

28. Shao X, Liu D, Martin T, *et al*. Measuring human placental blood flow with multidelay 3D GRASE pseudocontinuous arterial spin labeling at 3 T. *J Magn Reson Imaging*. 2018;47(6):1667-1676.

29. Armstrong T, Liu D, Martin T, *et al*. 3D Mapping of the placenta during early gestation using free-breathing multiecho stack-of-radial MRI at 3 T. *J Magn Reson Imaging*. 2019;49(1):291-303.

30. Martin T, Janzen C, Li X, *et al*. Characterization of uterine motion in early gestation using MRI-based motion tracking. *Diagnostics (Basel)*. 2020;10(10):840.

31. Hernando D, Kellman P, Haldar JP, Liang ZP. Robust water/fat separation in the presence of large field inhomogeneities using a graph cut algorithm. *Magn Reson Med*. 2010;63(1):79-90.

32. Lee B. Supplemental materials for utility of in-vivo magnetic resonance imaging in gestational diabetes mellitus during early pregnancy. *Zenodo*. Posted August 31, 2022. https://doi.org/10.5281/zenodo.7039057

33. Hedderson MM, Darbinian JA, Ferrara A. Disparities in the risk of gestational diabetes by race-ethnicity and country of birth. *Paediatr Perinat Epidemiol*. 2010;24(5):441-448.